ELSEVIER

Chemical Engineering Journal 120 (2006) 193–202

Chemical Engineering Journal

www.elsevier.com/locate/cej

Application of oxygen ion-conductive membranes for simultaneous electricity and hydrogen generation

Mikhail Granovskii, Ibrahim Dincer*, Marc A. Rosen

Faculty of Engineering and Applied Science, University of Ontario Institute of Technology, 2000 Simcoe Street North, Oshawa, Ont., Canada L1H 7K4

Received 30 June 2005; received in revised form 30 January 2006; accepted 31 January 2006

Abstract

The high temperature of the air in power generation gas-turbine cycles involving natural gas (mainly methane) oxidation accounts for the utilization of ion-conductive membranes within solid oxide fuel cells (SOFCs) and membrane reactors (MRs). In SOFCs, the electricity is directly derived from the chemical exergy of methane (SOFCs with internal methane reforming are considered here). Within a membrane reactor (MR), which is considered a substitute for combustion chambers in traditional gas-turbine units, the ion-conductive membranes separate oxygen from air and allow the flow of the hot combustion products (carbon dioxide and steam) to be separated from air. It permits the use of combustion products which are not diluted in nitrogen in the process of methane conversion into hydrogen. A modified gas-turbine cycle that includes a SOFC stack, an MR (instead of a traditional combustion chamber), and a catalytic reactor to convert methane to hydrogen is proposed. An exergy analysis of the proposed system is conducted to evaluate its exergy efficiency and the exergy losses for the processes occurring within the system. It is shown that, in comparison to the traditional gas-turbine cycle, there is a significant reduction (more than three times) in the exergy losses for the most irreversible process occurring in the system, natural gas combustion. It is also found that the proposed cogeneration scheme, including both power generation and the industrial catalytic conversion of methane to hydrogen, permits improved efficiencies for both technologies. The efficiency of this cogeneration, as well as the reduction in exergy losses, is demonstrated by the following observation: if the value of energy (exergy) efficiency of hydrogen production is considered equal to that for a traditional process, the corresponding thermal (energy) efficiency for electricity generation would reach values of 80–96% depending on the efficiency of a SOFC stack. The combined SOFC and MR application also eliminates the possibility of toxic nitrogen oxides formation and, at the same time, makes carbon dioxide removal from flue gases feasible (due to its high concentration). The development of the proposed technology is especially important, within the context of the hydrogen economy, if the produced hydrogen is used as a fuel for fuel cell vehicles.

Keywords: Solid oxide fuel cell; Energy; Exergy; Efficiency; Hydrogen; Electricity; Fuel cell

1. Introduction

Natural gas (mainly methane) combustion can be made less irreversible if (i) methane is preliminary converted into a mixture of carbon monoxide and hydrogen (a synthesis gas); (ii) this mixture is combusted in an atmosphere of the combustion products (carbon dioxide and steam); and (iii) some part of the synthesis gas is withdrawn from the mechanical power generation cycle [1,2]. Increasing efficiency so it approaches reversible conditions reduces the exergy losses and, as a result, leads to increases in energy and exergy efficiencies. Utilization of oxygen instead of air permits these gains, but it demands substantial extra expenses related to air separation. Industrial cryogenic air separation is characterized by extremely low energy efficiency (less than 15%) and is expensive.

The application of oxygen ion-conductive membranes allows unwanted expenses connected to the preliminary air separation to be avoided. The most distinctive feature of the oxygen ion-conductive membranes is that they are conductive to the negative charged ions of oxygen. This property accounts for their application as an electrolyte in solid oxide fuel cells (SOFCs). A neutral molecule of oxygen takes four electrons from the porous cathode of SOFCs (Fig. 1a), depletes into the negative charged ions, penetrates through the ion-conductive membrane, returns electrons to the external circuit, and oxidizes fuel (CH_4, H_2, CO) on the porous anode. In a membrane reactor (MR) (Fig. 1b) nearly the same process occurs but, in this case, the membrane con-

* Corresponding author. Tel.: +1 905 721 8668; fax: +1 905 721 3370.
E-mail addresses: mikhail.granovskiy@uoit.ca (M. Granovskii), ibrahim.dincer@uoit.ca (I. Dincer), marc.rosen@uoit.ca (M.A. Rosen).

1385-8947/$ – see front matter © 2006 Elsevier B.V. All rights reserved.
doi:10.1016/j.cej.2006.01.020

Nomenclature

a, b, c	molar flows
D	exergy losses
E	exergy
F	Faraday constant
G	Gibbs free energy
H	enthalpy
K	equilibrium constant
MR	membrane reactor
n	number of moles
N	total number of moles in a mixture
P	pressure
Q	heat
R	universal gas constant
S	entropy
SOFC	solid oxide fuel cell
T	temperature
V	voltage
W	work

Greek symbols

Δ	difference
η	efficiency

Subscripts

Air	air
c	methane converter
CH_4	methane
CO	carbon monoxide
CO_2	carbon dioxide
cmp	compressor
cold	cold flows
e	electricity, electrons
H_2	hydrogen
H_2O	water
hot	hot flows
i	index
ideal	ideal
in	input
LHV	lower heating value
max	maximum
min	minimum
mr	membrane reactor
out	output
p	pressure
Q	heat
real	real
R	steam-water Rankine cycle
s	SOFC stack
sg	synthesis gas
t	turbine
tr	heat transfer
T	thermal
w	mechanical work generation or consumption
0	reference environment

Superscripts

Air	air
c	methane converter
CH_4	methane
cmb	combustion products
cnv	conversion products
cold	cold flows
hot	hot flows
id	ideal
real	real
mr	membrane reactor
s	SOFC stack
0	reference environment
*	average

ducts both oxygen ions and electrons in the opposite directions. Therefore, such membranes are often called mixed conducting membranes. The transport of oxygen is based on ion diffusion so that the selectivity of these membranes is very high provided no pores and cracks are present. The difference between oxygen partial pressures at the opposite sides of a membrane is the driving force for oxygen separation [3]. This driving force in SOFCs and MRs is high, because the oxygen molecules oxidize fuels and quickly form other chemical species at the permeable side of the membrane.

Oxygen ion-conductive membranes are made of ceramic materials (usually zirconia oxides) and have good performance characteristics at temperatures higher than 700 °C. Therefore an SOFC stack is often introduced into traditional power generation cycles, where it operates at temperatures of 800–1100 °C (e.g. [4,5]). An MR is being developed for operation up to 1250 °C, as a substitute for combustion chambers in advanced zero-emission power plants (AZEP) (e.g. [6]). New materials for the anodes of SOFCs contain a catalyst for the methane reforming process, allowing methane conversion into a mixture of hydrogen and carbon monoxide directly on the surface of the anode [7,8]. SOFCs thereby become more flexible, compact and effective, and there is no need to perform a preliminary reforming of methane.

The purpose of this paper is to demonstrate that a combined application of SOFCs, MRs, and catalytic methane converters permits substantial improvements in the efficiency of natural gas conversion into electricity and hydrogen. A new design of a combined gas-turbine cycle with hydrogen generation is proposed.

2. The system—a combined gas-turbine cycle with hydrogen generation

A combined gas-turbine cycle with a hydrogen generation unit is presented in Fig. 2. The initial stream of natural gas, after heating in device 14 (in order to achieve after compression the temperature of combustion products) and compression in device 15, is divided into two flows. The first is mixed with combustion products (carbon dioxide and steam) and directed to

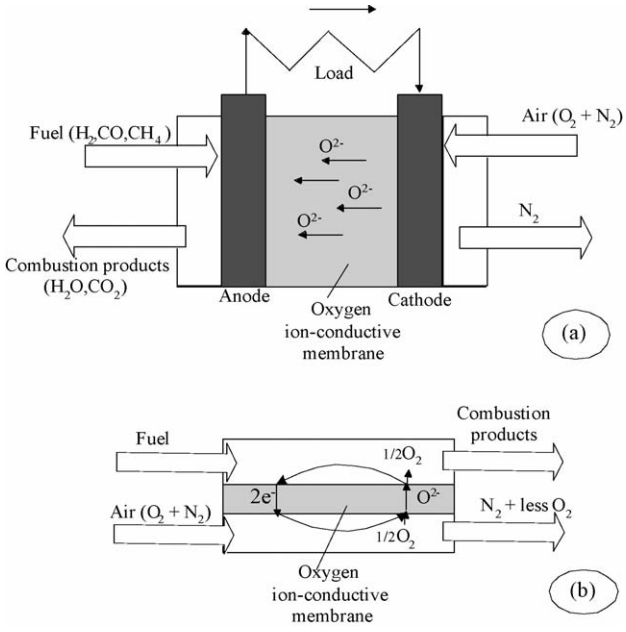

Fig. 1. (a) Application of oxygen ion-conductive membranes in a solid oxide fuel cell (SOFC) and (b) membrane reactor (MR) which is considered a replacement for the combustion chamber in a gas-turbine unit.

the anodes of the SOFC stack (device 4), where two processes occur simultaneously: conversion of methane into a mixture of carbon monoxide and hydrogen on the surface of the anodes and combustion of the resultant mixture with oxygen. The burning of oxygen is accompanied by electricity generation in the SOFCs. The gaseous mixture from the anodes (conversion and combustion products) is cooled in a heat exchanger (device 10),

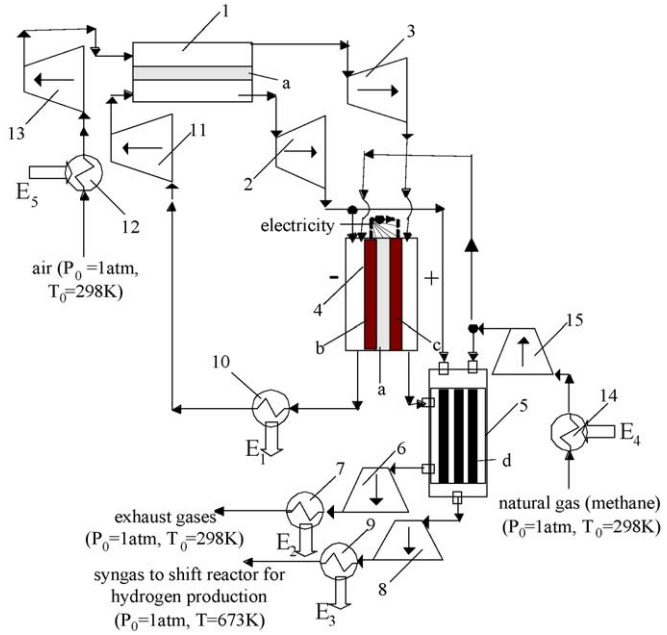

Fig. 2. An application of a SOFC and MR in a combined gas-turbine cycle with a hydrogen generation unit. Numbers indicate devices according to the following legend—1: MR; 2, 3, 6, 8: turbines; 11, 13, 15: compressors; 4: SOFC stack; 5: methane converter; 7, 9, 10, 12, 14: heat exchangers; a: oxygen ion-conductive membranes; b, c: anode and cathode of SOFC stack, respectively.

compressed in device 11, and directed to the MR (device 1), where the remainder of the conversion products combust in oxygen, and then expand in a turbine (device 2).

The combustion products are then divided into two flows. The first is mixed with the initial flow of methane and directed to the SOFC stack, while the other is mixed with the second flow of methane and enters the catalytic methane converter (device 5). After methane conversion to hydrogen and carbon monoxide in device 5, the gaseous mixture is expanded in a turbine (device 8), cooled in a heat exchanger (device 9) and directed to the shift reactor, where the remainder of the carbon monoxide and steam is converted to hydrogen.

Air is heated in device 12, compressed in device 13, directed to the MR (device 1), where some quantity of oxygen is transferred through the oxygen ion-conductive membrane and combusted with fuel. The air heating in device 12 is required in order to achieve after compression the temperature of the fuel flow which is directed, like air, to the MR.

The temperature of air reaches its maximum, and then the air is expanded in the turbine (device 3) and directed to the cathodes of the SOFCs (device 4). In the SOFCs, the air loses some of its oxygen, is heated and enters the space between pipes in the catalytic converter (device 5). In device 5, the heat of air is transferred to the reaction mixture in the pipes, and then expanded in the turbine (device 6), and cooled in the heat exchanger (device 7).

The power generation design combines a traditional gas-turbine cycle, which consists of compressors (devices 11 and 13), a combustion chamber (which is represented by the MR, device 1), and turbines (devices 2 and 3) with the SOFC stack (device 4) and methane converter (device 5). Heat exchangers are conditionally divided into the heat releasing (devices 7, 9 and 10) and heat receiving (devices 12 and 14) types. Mechanical work is produced in the turbines and consumed in the compressors. The work is transformed into electrical energy, which is also directly generated in the SOFC stack. The endothermic process of methane conversion to hydrogen (via a synthesis gas) in device 5 is introduced into the power generation cycle.

3. Thermodynamic modeling of the system

The general assumptions applied in the exergy analysis of the proposed design follow: (i) gases are modeled as ideal; (ii) energy losses due to mechanical friction are negligible; (iii) thermodynamic and chemical equilibria are achieved at the outlet of the SOFC stack and methane converter; and (iv) all combustible components are combusted completely in the MR.

The general parameters used in the combined power generation cycle are listed in Table 1. The parameters η_t, η_{cmp}, P_{max}, P_{min} and T_{max} are often cited (e.g. [9]).

3.1. Thermodynamic model of the SOFC stack

There are three mass and energy inputs to the SOFC stack (device 4): methane, combustion products and air, and three mass and energy outputs: products of methane conversion, electrical work W_e, and air. The composition of the gaseous flows along

Table 1
General parameter values for the combined power generation cycle (Fig. 2)

Parameter	Value
Isentropic efficiency of turbines, η_t	0.93
Isentropic efficiency of compressors, η_{cmp}	0.85
Energy efficiency of electricity generation in SOFC, η_s	0.5
Maximum pressure in the gas-turbine cycle, P_{max} (atm)	10
Minimum pressure in the gas-turbine cycle, P_{min} (atm)	1
Maximum temperature in the cycle (at the MR outlet), T_{max} (K)	1573
Temperature of fuel at the inlet of the SOFC stack, T_s (K)	1273
Temperature of fuel and air at the outlet of the SOFC stack, T_s (K)	1273
Ratio of methane combusted in the power generation cycle to the methane converted	1.0:0.7
Total amount of combustion products after MR (mol)	6
Ratio of amounts of combustion products directed to SOFC and methane converter	1:1
Standard temperature, T_0 (K)	298
Standard pressure, P_0 (atm)	1
Air composition (vol.%)	21% O_2, 79% N_2

the SOFC stack changes according to the reactions on the anode surface:

$$CH_4 + 2O_2 \rightarrow CO_2 + 2H_2O_{(g)} + 802.6\,kJ \quad (1)$$

$$CH_4 + H_2O \leftrightarrow CO + 3H_2 - 206\,kJ \quad (2)$$

$$CO + H_2O \leftrightarrow CO_2 + H_2 - 41\,kJ \quad (3)$$

According to assumption (iii), the composition of the reaction mixture at the SOFC stack outlet is determined by the equilibrium equations for reactions (2) and (3). The final concentration of reagents does not depend on the component (CH_4) chosen for burning with oxygen because the reactions:

$$H_2 + (1/2)O_2 \rightarrow H_2O, \qquad CO + (1/2)O_2 \rightarrow CO_2 \quad (4)$$

can be obtained as a linear combination of reactions (1)–(3).

The compositions of gaseous mixtures (fuel and air) at the end of the SOFC processes are defined by solving a system of chemical equilibrium and heat balance equations. The chemical equilibrium equations for reactions (2) and (3) follow:

$$K_{p1}(T_s) = \frac{P_{H_2}^3 P_{CO}}{P_{CH_4} P_{H_2O}} \quad (5)$$

$$K_{p2}(T_s) = \frac{P_{H_2} P_{CO_2}}{P_{CO} P_{H_2O}} \quad (6)$$

where T_s is the temperature at the SOFC stack inlet and outlet (Table 1), $K_{p1}(T_s)$ and $K_{p2}(T_s)$ are equilibrium constants, which depend only on temperature T_s and have been widely presented in the literature (e.g. [10]). The parameters P_{H_2}, P_{H_2O}, P_{CH_4}, P_{CO} and P_{CO_2} are partial pressures of reagents in the mixture at the outlet of the SOFC stack. The partial pressure of the ith component is

$$P_i = \frac{n_i}{N} P \quad (7)$$

where n_i is the number of moles of the ith component in the gaseous mixture, N the total number of moles in the mixture, and P is the pressure of the mixture.

The oxygen that permeates through the ion-conductive membrane from air is combusted (reaction (1)); the released heat is converted into electrical work W_e and heats the coming air and provides heat to promote the endothermic conversion of methane to hydrogen and carbon monoxide ((2) and (3)). Considering the SOFC stack as an adiabatic device, the following energy balance can be written:

$$\Delta H_s + W_e = 0 \quad (8)$$

Here W_e is the electrical energy, ΔH_s is the enthalpy change in the SOFC, expressible as

$$\Delta H_s = H_{out}^s - H_{in}^s \quad (9)$$

where

$$H_{in}^s = \sum b_i^{Air} H_i^{Air}(T_{Air}) + b_{CH_4} H_{CH_4}(T_s) + \sum b_i^{cmb} H_i^{cmb}(T_s) \quad (10)$$

$$H_{out}^s = \sum c_i^{Air} H_i^{Air}(T_s) + \sum c_i^{cnv} H_i^{cnv}(T_s) \quad (11)$$

and where H_{in}^s and H_{out}^s denote, respectively, the enthalpies of the input and output flows; H_i^{Air}, H_{CH_4}, H_i^{cmb}, and H_i^{cnv}, respectively, the enthalpies of air, methane, combustion products at the SOFC inlet, and conversion products at the SOFC outlet; T_{Air} the temperature of air at the inlet; T_s the temperature of the methane and combustion products at the SOFC inlet and air and conversion products at the SOFC outlet; b_i^{Air}, b_{CH_4} and b_i^{cmb} the molar flows of air, methane, and combustion products at the inlet; and c_i^{Air} and c_i^{cnv} denote the molar flows of air and conversion products at the SOFC outlet.

In Table 1 the efficiency of the SOFC is presented as a percentage of the Gibbs free energy change, in line with the following expression:

$$W_e = -\eta_s \Delta G_s \quad (12)$$

An electrical efficiency of unity means that the Gibbs free energy change ΔG_s in the SOFC stack is equal to the useful electrical energy W_e. In Eq. (12), ΔG_s is the free energy difference between the output and input flows, expressible as

$$\Delta G_s = G_{out}^s - G_{in}^s \quad (13)$$

where

$$G_{in} = \sum b_i^{Air} G_i^{Air}(T_{Air}) + b_{CH_4} G_{CH_4}(T_s) + \sum b_i^{cmb} G_i^{cmb}(T_s) \quad (14)$$

$$G_{out} = \sum c_i^{Air} G_i^{Air}(T_s) + \sum c_i^{cnv} G_i^{cnv}(T_s) \quad (15)$$

and where G^{s}_{out} and G^{s}_{in} are the free energies of input and output flows; and G_i^{Air}, G_{CH_4}, G_i^{cmb} and G_i^{cnv} are the free energies of air, methane, combustion products and conversion products, respectively. The free energy of a component in a gaseous mixture is written as follows:

$$G_i = H_i(T) - TS_i(T) \tag{16}$$

$$S_i(T) = S_i^0(T) - R\ln P_i \tag{17}$$

where $H_i(T)$ and $S_i^0(T)$ are the enthalpy and entropy of a component at $P_0 = 1$ atm (note that the enthalpy of an ideal gas does not depend on pressure), P_i is the partial pressure, T is the temperature, and R is the universal gas constant. The dependences of H_i and S_i^0 on T are given in reference books (e.g. [11]).

The quantity of oxygen combusted and the composition of conversion products are found by numerical solution of Eqs. (5), (6), (8) and (12), taking into account Eqs. (9)–(11) and (13)–(15).

The exergy losses D_s represent losses of an ability to produce useful work caused by process irreversibilities. These losses are equal to the entropy generation ΔS in a device multiplied by the temperature of the reference environment T_0 (by the Gouy and Stodola formula). Thus, the exergy losses in the SOFC stack D_s are equal to

$$D_s = T_0 \Delta S_s \tag{18}$$

where

$$\Delta S_s = S^s_{out} - S^s_{in} \tag{19}$$

$$S^s_{in} = \sum b_i^{Air} S_i^{Air}(T_{Air}) + b_{CH_4} S_{CH_4}(T_s) + \sum b_i^{cmb} S_i^{cmb}(T_s) \tag{20}$$

$$S^s_{out} = \sum c_i^{Air} S_i^{Air}(T_s) + \sum b_i^{cnv} S_i^{cnv}(T_s) \tag{21}$$

and where ΔS_s is the entropy generation in the SOFC stack; S^s_{in} and S^s_{out} the entropies of the input and output flows; S_i^{Air}, S_{CH_4}, S_i^{cmb} and S_i^{cnv} the entropies of air, methane, combustion products and conversion products, respectively; and T_0 is the temperature of the reference environment (Table 1). Entropies of components are calculated in line with the expression in Eq. (17).

3.2. Thermodynamic model of methane converter

There are three input flows to the methane converter: methane, combustion products (the mix of methane and combustion products constitutes the reaction mixture), and air; and there are two output flows: products of methane conversion and cooled air. The composition of the reaction mixture through the catalytic reactor (device 5) changes according to the catalytic reactions of methane conversion (Eqs. (2) and (3)). According to assumption (iii), the final composition of the reaction mixture is determined by the chemical equilibrium expressed by Eqs. (5) and (6), where equilibrium constants $K_{p1}(T_s)$, $K_{p2}(T_s)$ are calculated for the temperature at the converter outlet T_c. The unknown final composition of the reaction mixture and temperature T_c are determined by solving the equilibrium equations (5) and (6) together with the heat balance equations.

The heat balance for the adiabatic converter is as follows:

$$\Delta H_c = 0 \tag{22}$$

where ΔH_c is the enthalpy change in the methane converter:

$$\Delta H_c = H^c_{out} - H^c_{in} \tag{23}$$

$$H^c_{in} = \sum c_i^{Air} H_i^{Air}(T_s) + c_{CH_4} H_{CH_4}(T_s) + \sum c_i^{cmb} H_i^{cmb}(T_s) \tag{24}$$

$$H^c_{out} = \sum c_i^{Air} H_i^{Air}(T_c) + \sum c_i^{cnv} H_i^{cnv}(T_c) \tag{25}$$

Here H^c_{in} and H^c_{out} are, respectively, the enthalpies of the input and output flows; H_i^{Air}, H_{CH_4}, H_i^{cmb} and H_i^{cnv} the enthalpies of air, methane, combustion products at the input, and conversion products at the output, respectively; T_s the temperature of air (after the SOFC stack), methane and combustion products at the inlet; T_c the temperature of air and conversion products at the outlet; c_{CH_4}, c_i^{cmb} the molar flows of methane and combustion products at the inlet, respectively; c_i^{Air} the molar flow of air components at the inlet and outlet of the converter; and c_i^{cnv} is the molar flow of conversion products at the outlet of the reactor.

After calculating the composition of the reaction mixture c_i^{cnv} and the temperature T_c at the outlet of the converter, the exergy losses and entropy generation ΔS_c are evaluated according to the following expressions:

$$D_c = T_0 \Delta S_c \tag{26}$$

$$\Delta S_c = S^c_{out} - S^c_{in} \tag{27}$$

$$S^c_{in} = \sum c_i^{Air} S_i^{Air}(T_s) + c_{CH_4} S_{CH_4}(T_s) + \sum c_i^{cmb} S_i^{cmb}(T_s) \tag{28}$$

$$S^c_{out} = \sum c_i^{Air} S_i^{Air}(T_c) + \sum c_i^{cnv} S_i^{cnv}(T_c) \tag{29}$$

where ΔS_c is the entropy generation in the methane converter; S^c_{in} and S^c_{out} the entropies of the input and output flows, respectively; S_i^{Air}, S_{CH_4}, S_i^{cmb} and S_i^{cnv} the entropies of air, methane, combustion products and conversion products, respectively; and T_0 is the temperature of the reference environment (Table 1).

3.3. Thermodynamic model of membrane reactor (MR)

There are two flows into the MR: the flow of the initial "fresh" air and the flow of conversion products after the SOFC. Also, there are two output flows: combustion products and air with a reduced content of oxygen. According to assumption (iv) in the third section of this paper, the quantity of oxygen consumed is that needed for complete burning of the combustible components which are leaving the SOFC stack: CH_4, H_2, CO. Thus, the composition of the combustion products and the quantity of oxygen permeating through the ion-conductive membrane are

determined by the SOFC-stack performance. The temperature T_r at the input of the MR is evaluated by solving the system of heat balance equations at a given T_{max} (the maximum temperature in the cycle in Table 1).

Since the MR is adiabatic, the heat balance is expressible as

$$\Delta H_{mr} = 0 \tag{30}$$

where ΔH_r is the enthalpy change in the MR:

$$\Delta H_{mr} = H_{out}^{mr} - H_{in}^{mr} \tag{31}$$

$$H_{in}^{mr} = \sum a_i^{Air} H_i^{Air}(T_r) + \sum b_i^{cnv} H_i^{cnv}(T_r) \tag{32}$$

$$H_{out}^{mr} = \sum b_i^{Air} H_i^{Air}(T_{max}) + \sum (b_i^{cmb} + c_i^{cmb}) H_i^{cmb}(T_{max}) \tag{33}$$

where H_{in}^{mr} is the enthalpy of the input flows; H_{out}^{mr} the enthalpy of the output flows; H_i^{Air}, H_i^{cnv} and H_i^{cmb} the enthalpies of the air, conversion products, and combustion products, respectively; T_r the temperature of air and conversion products at the input; T_{max} the temperature of air and combustion products at the output (the maximum temperature in the cycle, see Table 1); a_i^{Air}, b_i^{cnv} the molar flows of air components and conversion products at the input, respectively; and b_i^{Air}, $b_i^{cmb} + c_i^{cmb}$ are the molar flows of air components and the total flow of combustion products at the output, respectively (b_i^{cmb} is directed to the SOFC stack, c_i^{cmb} is directed to the methane converter).

The exergy losses due to internal irreversibility D_{mr} are calculated using the Gouy and Stodola formula:

$$D_{mr} = T_0 \Delta S_{mr} \tag{34}$$

where

$$\Delta S_{mr} = S_{out}^{mr} - S_{in}^{mr} \tag{35}$$

$$S_{in}^{mr} = \sum a_i^{Air} S_i^{Air}(T_r) + \sum b_i^{cnv} S_i^{cnv}(T_r) \tag{36}$$

$$S_{out}^{mr} = \sum a_i^{Air} S_i^{Air}(T_{max}) + \sum (b_i^{cmb} + c_i^{cmb}) S_i^{cmb}(T_{max}) \tag{37}$$

Here S_i^{Air}, S_i^{cnv}, S_i^{cmb} are the entropies of air, conversion products, and combustion products, respectively.

3.4. Thermodynamic model of adiabatic turbines and compressors

Mechanical work produced in adiabatic turbines (or consumed in adiabatic compressors) is equal to

$$W = \Delta H_w(T_{in}, T_{out}) \tag{38}$$

Here T_{in} is the temperature of gaseous mixture at the inlet of a turbine (compressor), T_{out} the temperature of the gaseous mixture at the outlet of a turbine (compressor), and ΔH_w is the enthalpy difference between the output and input flows.

The exergy losses D_w in adiabatic turbines and compressors (there is no external heat exchange) is equal to

$$D_w = T_0 \Delta S_w \tag{39}$$

where ΔS_w is the entropy difference of the inlet and outlet flows (entropy generation).

An ideal turbine or compressor can be considered a device where the exergy losses equal zero:

$$\Delta S_w^{id}(T_{in}, P_{in}, T_{out}, P_{out}) = 0 \tag{40}$$

where P_{in} and P_{out} are the pressures of gaseous mixture at the inlet and outlet of a turbine (compressor), respectively.

The actual or real work W_{real} and the exergy losses D_w can be calculated as follows. First, one of the thermodynamic parameters, e.g., T_{in}^{ideal}, is obtained with Eq. (40), when the other three are given. Then T_{in}^{ideal} is substituted into Eq. (38) and the work of an ideal turbine (compressor) W_{ideal} is calculated. Applying the isentropic efficiencies, the real work is obtained as follows:

$$W_{real} = W_{ideal}\eta_t \quad \text{for turbines} \tag{41}$$

$$W_{real} = \frac{W_{ideal}}{\eta_{cmp}} \quad \text{for compressors} \tag{42}$$

The parameter W_{real} from Eq. (41) or (42) is substituted into Eq. (38), and T_{in}^{real} is evaluated. Finally, T_{in}^{real} is used to evaluate the entropy generation ΔS_w and the exergy losses D_w using Eq. (39).

3.5. Thermodynamic model of heat exchange processes

Any heat transfer from heating to heated flows is accompanied by exergy losses D_{tr} because there is a finite temperature difference between these flows. For a heating flow at a temperature above that of the reference environment, the exergy of the heating flow E_Q^{hot} is the maximum useful work which can be obtained in the ideal Carnot cycle where this flow is used as a heat source and the reference environment is the heat sink and can be expressed as

$$E_Q^{hot} = Q_{hot}\left(1 - \frac{T_0}{T_{hot}^*}\right) \tag{43}$$

where Q_{hot} is the heat transferred from the heating flow at a temperature T_{hot}^*, and T_0 is the temperature of the reference environment (often taken to be at 298 K). When the temperature at which heat is transferred out of the heating flow changes, from an initial temperature T_{max}^{hot} to a final temperature T_{min}^{hot}, an average value of T_{hot}^* can be used. This average temperature can be evaluated as the equivalent temperature at which the heat Q_{hot} is transferred with the same the enthalpy change ΔH_{ex}^{hot} and entropy change ΔS_{ex}^{hot} for the heating fluid, and expressed as

$$Q_{hot} = -\Delta H_{hot} \tag{44}$$

$$T_{hot}^* = \frac{\Delta H_{hot}}{\Delta S_{hot}} \tag{45}$$

When the temperature of the heated flow increases, from T_{min}^{cold} to T_{max}^{cold}, the equivalent average temperature at which the heat is

transferred can be evaluated similarly as

$$T^*_{\text{cold}} = \frac{\Delta H_{\text{cold}}}{\Delta S_{\text{cold}}} \tag{46}$$

and the exergy transfer associated with the heat transfer into the heated flow is expressible as

$$E^{\text{cold}}_{\text{Q}} = Q_{\text{cold}} \left(1 - \frac{T_0}{T^*_{\text{cold}}}\right) \tag{47}$$

where

$$Q_{\text{cold}} = \Delta H_{\text{cold}} \tag{48}$$

Net heat exchange will only occur from the heating to the heated flow if $T^*_{\text{hot}} > T^*_{\text{cold}}$ and the exergy losses D_{tr} caused by the irreversibility of the heat exchange process are expressible as

$$D_{\text{tr}} = Q_{\text{cold}} \left(\left(1 - \frac{T_0}{T^*_{\text{hot}}}\right) - \left(1 - \frac{T_0}{T^*_{\text{cold}}}\right)\right) \tag{49}$$

and the remainder (thermal) exergy ΔE of the heating flows is

$$\Delta E_{\text{T}} = (Q_{\text{hot}} - Q_{\text{cold}}) \left(1 - \frac{T_0}{T^*_{\text{hot}}}\right) \tag{50}$$

If there are several heating and heated flows in the system, enthalpy and entropy changes are calculated as the sum of the respective thermodynamic parameters of the flows.

3.6. Exergy balance of the overall system

An exergy balance of a system permits evaluation of the efficiency with which input energy flows are utilized. For the power generation scheme presented in Fig. 2 the exergy balance can be expressed as

$$\Delta E = E_{\text{in}} - E_{\text{out}} = \sum W_i + \Delta E_{\text{T}} + \sum D_i \tag{51}$$

where E_{in} is the sum of the exergies of the input methane and air at the standard conditions (T_0, P_0) as pointed in Fig. 2:

$$E_{\text{in}} = (b_{\text{CH}_4} + c_{\text{CH}_4})(H_{\text{CH}_4}(T_0) - T_0 S_{\text{CH}_4}(T_0, P_0)) + \sum a_i^{\text{Air}}(H_i^{\text{Air}}(T_0) - T_0 S_i^{\text{Air}}(T_0, P_0)) \tag{52}$$

Here E_{out} is the exergy of conversion products (synthesis gas) directed to a shift converter at the temperature $T_{\text{sg}} = 673$ K:

$$E_{\text{out}} = \sum c_i^{\text{cnv}}(H_i^{\text{cnv}}(T_{\text{sg}}) - T_0 S_i^{\text{cnv}}(T_{\text{sg}}, P_0)) \tag{53}$$

Here $\sum W_i$ is the sum of works generated in the turbines and in SOFCs, and consumed in the compressors (with a negative sign), ΔE_{T} the thermal exergy, and $\sum D_i$ is the sum of the exergy losses in the devices of the system.

The lower the exergy losses, the better is the exergy efficiency. If the material and energy inputs are the same in different power generation schemes, the most efficient one is characterized by lower exergy losses.

Table 2
Thermodynamic parameters of the fuel (methane) flow as it is converted in the combined gas-turbine cycle (Fig. 2)

Device number in Fig. 2	Direction	T (K)	P (atm)	Composition[a] (mol)				
				CH_4	H_2O	H_2	CO	CO_2
1	Input	1261	10.0	~0.0	3.46	0.54	0.42	1.58
	Output	1573	10.0	~0.0	4.0	0.0	0.0	2.0
2	Input	1573	10.0	~0.0	4.0	0.0	0.0	2.0
	Output	1273	2.53	~0.0	4.0	0.0	0.0	2.0
4	Input	1273	2.53	1.0	2.0	0.0	0.0	1.0
	Output	1273	2.53	~0.0	3.46	0.54	0.42	1.58
10	Input	1273	2.53	~0.0	3.46	0.54	0.42	1.58
	Output	974	2.53	~0.0	3.46	0.54	0.42	1.58
11	Input	974	2.53	~0.0	3.46	0.54	0.42	1.58
	Output	1261	10.0	~0.0	3.46	0.54	0.42	1.58
5	Input	1273	2.53	0.7	2.0	0.0	0.0	1.0
	Output	1021	2.53	0.02	1.48	1.88	0.84	0.84
8	Input	1021	2.53	0.02	1.48	1.88	0.84	0.84
	Output	833	1.0	0.02	1.48	1.88	0.84	0.84
9	Input	833	1.0	0.02	1.48	1.88	0.84	0.84
	Output	673	1.0	0.02	1.48	1.88	0.84	0.84
14	Input	298	1.0	1.7	0.0	0.0	0.0	0.0
	Output	1133	1.0	1.7	0.0	0.0	0.0	0.0
15	Input	1133	1.0	1.7	0.0	0.0	0.0	0.0
	Output	1273	2.53	1.7	0.0	0.0	0.0	0.0

[a] The flow composition is given per mole of methane combusted in the power generation cycle.

Table 3
Thermodynamic parameters of air as it flows through the combined gas-turbine cycle (Fig. 2)

Device number in Fig. 2	Direction	T (K)	P (atm)	Composition[a] (mol)	
				O_2	N_2
1	Input	1261	10.0	3.15	11.85
	Output	1573	10.0	2.67	11.85
3	Input	1573	10.0	2.67	11.85
	Output	1162	2.53	2.67	11.85
4	Input	1162	2.53	2.67	11.85
	Output	1273	2.53	1.15	11.85
5	Input	1273	2.53	1.15	11.85
	Output	1021	2.53	1.15	11.85
6	Input	1021	2.53	1.15	11.85
	Output	819	1.0	1.15	11.85
7	Input	819	1.0	1.15	11.85
	Output	298	1.0	1.15	11.85
12	Input	298	1.0	3.15	11.85
	Output	599	1.0	3.15	11.85
13	Input	599	1.0	3.15	11.85
	Output	1261	10.0	3.15	11.85

[a] The flow composition is given per mole of methane combusted in the power generation cycle.

4. Results and discussion

An application is presented of ion-conductive membranes within SOFCs and MR, which allows the flow of the hot combustion products (carbon dioxide and steam) to be separated from air, and to combine power and hydrogen generation processes (carbon dioxide and steam are the initial reagents for the methane conversion reaction (2)). To describe the advantages of this combination, a thermodynamic analysis of a combined gas-turbine cycle with a hydrogen generation unit (Fig. 2) is performed. The results are presented in Tables 2–5. Tables 2 and 3 list thermodynamic parameter values for the fuel (methane) and air flows within the combined gas-turbine cycle (Fig. 2). Using these data, mechanical and electrical work values and the exergies of released and absorbed heat are evaluated. Table 4 presents mechanical and electrical work generated in the turbines and SOFC stack, the mechanical work consumed in compressors (with a negative sign), and the exergy losses accompanying these processes.

Table 4
Generated work and exergy losses for the processes in the combined gas-turbine cycle (Fig. 2)[a]

Device number in Fig. 2	W (kJ)	D (kJ)
2	89.7	1.6
3	207.1	4.1
4	497.4	29.4
6	85.0	2.3
8	35.6	0.2
11	−89.8	4.2
13	−324.4	22.3
15	−18.8	0.7
Total	481.8	64.8

[a] Data are given per mole of methane combusted in the power generation cycle.

Table 5
Exergy losses in the MR and methane converter[a]

Device number in Fig. 2	D (kJ)
1	27.6
5	15.9
Methane mixing	10.0
Total	53.5

[a] Data are given per mole of methane combusted in the power generation cycle.

Table 5 presents the exergy losses in the MR and methane converter. Table 6 provides the heats Q and thermal exergies E_Q of the heating and heated flows (with a negative sign) in the system. A heat transfer ($Q_{cold} = 270$ kJ) from the heating flows at $T^*_{hot} = 630$ K (the equivalent absolute temperature of the heat transfer) to the heated flows at $T^*_{cold} = 520$ K (the equivalent

Table 6
Input and output thermal energy and thermal exergy values for the system[a]

Device number in Fig. 2	E_Q (kJ)	Q (kJ)
7	87.7	205.5
9	17.7	29.3
10	67.5	92.9
Total output	172.9	327.7
12	−41.9	−134.7
14	−46.2	−82.3
Total input	−88.1	−217.0

[a] Data are given per mole of methane combusted in the power generation cycle.

Table 7
Characteristics of the heat transfers in the system (Fig. 2)[a]

Q_{cold} (kJ)	217.0
$Q_{hot} - Q_{cold}$ (kJ)	110.7
ΔE_T (kJ)	58.4
D_{tr} (kJ)	26.3
W_R (kJ)	35.0
D_R (kJ)	23.4
T^*_{cold} (K)	502
T^*_{hot} (K)	630

[a] Data are given per mole of methane combusted in the power generation cycle.

absolute temperature of the total input heat) is accompanied by the exergy losses D_{tr}. The characteristics of the heat transfer from the heating to heated flows are presented in Table 7.

The thermal exergy ΔE_T can be converted into mechanical work in a bottoming steam-water (Rankine) cycle (not shown in Fig. 2) with an exergy efficiency (η_R) of about 60% [12], so that

$$W_R = \eta_R \Delta E_T \quad \text{and} \quad D_R = \Delta E_T - W_R \tag{54}$$

After substituting W_R and D_R into Eq. (51) instead of ΔE_T, the exergy change $\Delta E = 684.8$ kJ in the system is distributed only between work W and the exergy losses D.

A comparison of the exergy balances of the presented system with a traditional gas-turbine unit with a bottoming steam cycle (using exergy characteristics from [2]) is presented in Fig. 3. The exergy losses from methane oxidation in a SOFC and an MR are about three times lower than those in the combustors of traditional gas-turbine plants, while the sum of other exergy losses (mixing, heat exchange, etc.) are almost equal in both cases. The exergy efficiency for electricity production in the presented scheme is about 0.75 comparing to 0.54 for a traditional combined gas-turbine unit.

To clarify the advantages of hydrogen generation within the power generation cycle, as well as the reduction in associated

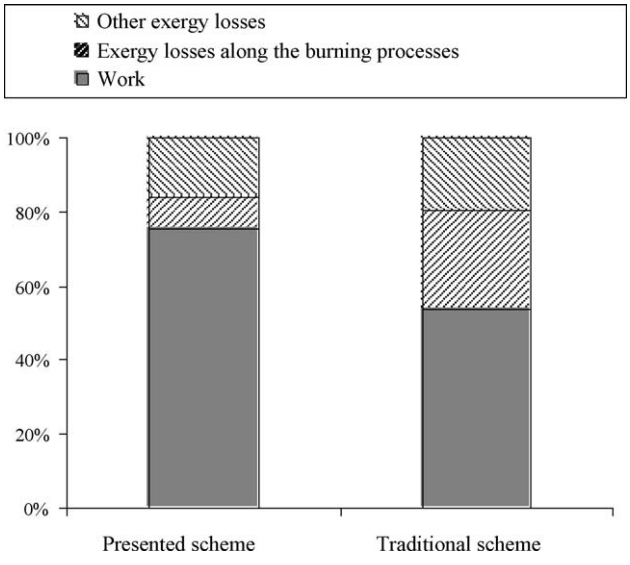

Fig. 3. Comparison of the exergy balance of the system in Fig. 2 with the exergy balance [2] of a traditional gas-turbine unit combined with a bottoming steam cycle.

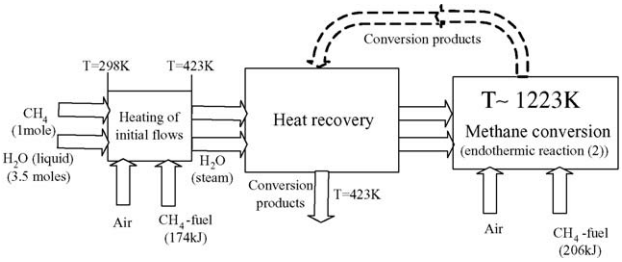

Fig. 4. Simplified schematic of the heat transfer associated with the process of methane conversion.

exergy losses, we compare the efficiency of the system considered with a traditional combined gas-turbine cycle on an energy basis. A simplified illustration of the heat transfers associated with the traditional process of methane conversion is presented in Fig. 4. The source of the heat is methane (natural gas) combustion. So as one flow of methane is combusted, another is mixed with steam to be converted into hydrogen as a synthesis gas. Methane is mixed with steam in a ratio of 1:3.5 on a molar basis and directed into a methane converter. As mentioned by Hinderink et al. [13], for technical reasons the heat streams below 150 °C (423 K) are not used for heat recovery in this process. As illustrated in Fig. 4, the heat required to evaporate water (154 kJ), to increase the gaseous flows temperatures (20 kJ), and to carry out the endothermic reaction of methane conversion (206 kJ) can be considered as a rough estimation of the methane combusted to provide the heat for the overall process.

To convert 0.7 mol of methane by means of traditional technology, the following quantity of methane should be supplied as fuel:

$$n_{CH_4} = 0.7 \frac{174\,\text{kJ} + 206\,\text{kJ}}{Q^{CH_4}_{LHV}} = 0.331 \tag{55}$$

where $Q^{CH_4}_{LHV} = 802.6$ kJ is the lower heating value of methane. In a separate analysis by Rosen [14], 0.5 mol of methane fuel was required to convert 1 mol methane.

The calculation in Eq. (55) means that 0.331 mol of methane fuel should be combusted to convert 0.7 mol of methane or 1.031 mol is consumed in the process of hydrogen generation. If the value of energy (exergy) efficiency of hydrogen production in the presented scheme (Fig. 2) is considered equal to that for a traditional process, as estimated below, the quantity of methane used in the power generation cycle should be reduced by 0.331. Taking into account the above result, a thermal efficiency for electricity generation in the presented scheme is equal to

$$\eta_T = \frac{W}{(1 - 0.331) Q^{CH_4}_{LHV}} = \frac{516.8}{(1 - 0.331) \times 802.6} = 0.96 \tag{56}$$

As a result of introducing SOFCs, MR and hydrogen production technology in a combined gas-turbine cycle, the thermal (energy) efficiency is increased from 0.55 (e.g. [15]) to 0.96. There are two reasons for this extraordinary improvement. First, there is a large reduction of the exergy losses for the most irreversible process occurring in the system, natural gas combustion, and, second, methane is not used as fuel for the endothermic process of methane conversion into synthesis gas (a mixture of hydrogen and carbon monoxide).

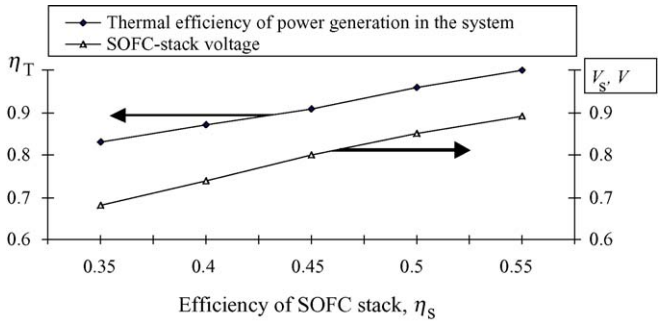

Fig. 5. Variation with SOFC stack energy efficiency η_s of thermal (energy) efficiency η_T of the gas-turbine cycle as a result of combining it with the methane conversion process, and the voltage of the SOFC stack V_s.

The operational circuit voltage in the SOFC stack can be evaluated as

$$V_s = -\frac{\eta_s \Delta G_s}{n_e F} = \frac{W_e}{n_e F} \quad (57)$$

where n_e is the number of moles of electrons transmitted into a circuit chain (requiring that 4 moles of electrons be multiplied by the total number of moles of oxygen penetrated through the ion conductive membrane), and F is the Faraday constant (the charge of 1 mol of electrons).

According to the data in Table 3 (row 4), for $\eta_s = 0.5$, per 1 mol of methane, 1.52 mol of oxygen is combusted in the SOFC stack, and each mole of oxygen releases four moles of electrons into an external circuit (Fig. 1a). Substituting these data into Eq. (57), a voltage $V_s = 0.85$ V for the SOFC stack is obtained. Fig. 5 presents the voltage of the SOFC stack V_s and a thermal (energy) efficiency η_T of the presented system as a function of η_s. Fig. 5 shows that a reduction in SOFC-stack efficiency leads to a decline in both the voltage of the SOFC stack and the thermal efficiency of the system. The voltage range 0.7–0.85 V seems quite realistic of the SOFC stack (e.g. [7]).

5. Conclusions

The application of oxygen ion-conductive membranes in a SOFC and a MR, and their utilization in a modified gas-turbine cycle combined with a methane conversion process to produce simultaneously electricity and hydrogen, leads to a significant reduction (more than three times), compared to a traditional gas-turbine cycle, in the exergy losses for the most irreversible process within the system, natural gas combustion. The proposed combination of power generation and hydrogen production technologies in one unit permits improved efficiencies of both. The efficiency of this cogeneration, as well as the reduction in exergy losses, is demonstrated by the following observation: if the value of energy (exergy) efficiency of hydrogen production is considered equal to that for a traditional process, the corresponding thermal (energy) efficiency for electricity generation would reach values of 80–96% depending on the SOFC stack efficiency.

The combined SOFCs and MR application also allows the flow of the hot combustion products (carbon dioxide and steam) to be separated from air, thereby eliminating the possibility of toxic nitrogen oxides formation and, at the same time, making carbon dioxide removal from flue gases feasible (due to its high concentration). This can be accomplished by means of well-known technologies (e.g., monoethanolamine purification or pressure swing adsorption).

The development of the proposed technology is especially important, within the context of the hydrogen economy, if the produced hydrogen used as a fuel for fuel cell vehicles.

Acknowledgements

The financial support of an Ontario Premier's Research Excellence Award, the Natural Sciences and Engineering Research Council of Canada and University of Ontario Institute of Technology is gratefully acknowledged.

References

[1] M. Granovskii, M. Safonov, S. Pozharskii, Integrated scheme of natural gas usage with minimum production of entropy, Can. J. Chem. Eng. 80 (2002) 998–1001.
[2] M. Granovskii, M. Safonov, New integrated scheme of the closed gas turbine cycle with synthesis gas production, Chem. Eng. Sci. 58 (2003) 3913–3921.
[3] A. Smith, J. Klosek, A review of air separation technologies and their integration with energy conversion processes, Fuel Process. Technol. 70 (2001) 115–134.
[4] P. Kuchonthara, S. Bhattacharya, A. Tsutsumi, Combinations of solid oxide fuel cell and several enhanced gas turbine cycles, J. Power Sources 124 (2003) 65–75.
[5] S. Chan, H. Ho, Y. Tian, Modelling of simple hybrid solid oxide fuel cell and gas turbine power plant, J. Power Sources 109 (2002) 111–120.
[6] S. Sundkvist, T. Griffin, N. Thourshaug, AZEP: development of an integrated air separation membrane—gas turbine, Report, Second Nordic Minisymposium on Carbon Dioxide Capture and Storage, Goteborg, 2001. Via http://www.entek.chalmers.se/~any/symp/symp2001.html (accessed on 15 April 2005).
[7] A. Weber, B. Sauer, A. Muller, D. Herbstritt, E. Ivers-Tiffee, Oxidation of H_2, CO and methane in SOFCs with Ni/YSZ-cermet anodes, Solid State Ionics 152–153 (2002) 543–550.
[8] K. Eguchi, H. Kojo, T. Takeguchi, R. Kikuchi, K. Sasaki, Fuel flexibility in power generation by solid oxide fuel cells, Solid State Ionics 152–153 (2002) 411–416.
[9] V. Kirillin, V. Sychev, A. Sheindlin, Engineering Thermodynamics, Nauka, Moscow, 1979.
[10] E.P. Melnikov (Ed.), Reference Book for Industrial Workers in Ammonia Industry, Himiya, Moscow, 1987.
[11] K.P. Mischenko, A.A. Ravdel (Eds.), Brief Reference Book of Physical and Chemical Values, Himiya, Moscow, 1981.
[12] Y. Cengel, R. Turner, Fundamentals of Thermal-fluid Science, 2nd ed., McGraw-Hill, New York, 2005.
[13] A. Hinderink, F. Kerkhof, A. Lie, J. Arons, H. Kooi, Exergy analysis with a flowsheeting simulator. II. Application: synthesis gas production from natural gas, Chem. Eng. Sci. 51 (1996) 4701–4715.
[14] M.A. Rosen, Comparative assessment of thermodynamic efficiencies and losses for natural gas-based production processes for hydrogen, ammonia and methanol, Energy Convers. Manage. 37 (1996) 359–367.
[15] G.G. Ol'hovskiy, Gas turbines in power generation industry, Teploenergetika 43 (1996) 2–11.